Long vs short-term synaptic learning rules after optogenetic spike-timing-dependent plasticity

Margarita Anisimova, Bas van Bommel, Marina Mikhaylova, J. Simon Wiegert, Thomas G. Oertner†, Christine E. Gee†*

Center for Molecular Neurobiology Hamburg, University Medical Center Hamburg-Eppendorf, Hamburg, Germany.

† These authors contributed equally to this work

* Corresponding author: Christine E. Gee

Email: christine.gee@zmnh.uni-hamburg.de

Keywords: Synaptic plasticity, hippocampus, optogenetics, LTP, LTD.

Author Contributions: Conceptualization, CEG, TGO, JSW; **Investigation,** MA, BvB, CEG; **Writing – Original Draft,** CEG, TGO, MA; **Writing – Review and Editing,** CEG, TGO, MA, BvB, JSW, MM; **Technical expertise,** TGO, CEG, MM; **Visualization,** MA, CEG, TGO; **Supervision,** CEG, TGO; **Project Funding Acquisition,** CEG, JSW. All authors approved the author list and final version.

This PDF file includes:

Main Text,
Figures 1 to 4
Supplementary Figures S1 to S6

Abstract

Spike-timing-dependent plasticity (STDP) is a candidate mechanism for information storage in the brain. However, it has been practically impossible to assess the long-term consequences of STDP because recordings from postsynaptic neurons last at most one hour. Here we introduce a new method to optically induce STDP (oSTDP), based on the spectrally distinct channelrhodopsins ChrimsonR and CheRiff. Selective expression in pre- and postsynaptic neurons allowed us to assess the strength of Schaffer collateral synapses up to 3 days after plasticity induction. When assessed during patch-clamp recordings, oSTDP followed classic STDP rules: Synapses potentiated (tLTP) when postsynaptic spikes followed presynaptic spikes (causal pairing) and depressed (tLTD) when postsynaptic spikes were first (anti-causal pairing). Surprisingly, three days after inducing oSTDP, only tLTP was evident regardless of the pairing sequence. This late potentiation depended on NMDA receptors and spontaneous activity was necessary in the two days following oSTDP. Our findings indicate that STDP induces changes in synaptic strength that persist to behaviorally relevant timescales. In addition, our data reveal a novel richness in STDP

dynamics and that tLTD at hippocampal Schaffer collateral synapses may be a transitory phenomenon.

Introduction

Attractive models of how memories form are based on observations that the strength of synapses change after coincident activity in the pre- and postsynaptic neurons, a process commonly referred to as spike-timing-dependent plasticity (STDP) (1–5). Indeed, STDP learning rules are now widely used for unsupervised learning and have been implemented to run on neuromorphic hardware (see e.g. 5–7). Timing-dependent long-term potentiation (tLTP) occurs when excitatory synaptic responses repeatedly precede postsynaptic action potentials, i.e. causal or Hebbian pairing. In contrast, timing-dependent long-term depression (tLTD) occurs when synaptic responses follow the postsynaptic action potentials, i.e. anti-causal pairing (9–11). However, STDP experiments are usually limited to 20-60 minutes, a period clearly not relevant for most forms of memory. This time limitation arises from the invasive nature of intracellular recordings, which are necessary to control postsynaptic spiking. In contrast, studies of synaptic plasticity using extracellular recordings to stimulate presynaptic axons and record ensemble responses from postsynaptic neurons can last several hours and even weeks when performed in vivo (12). Such studies have reported major differences in the mechanisms underlying early (~1-3 hours) and late (> 3 hours) LTP following short periods of intense presynaptic stimulation. For example, early hippocampal CA3-CA1 LTP depends on NMDA receptor activation, calcium-calmodulin dependent kinase II and the phosphorylation and postsynaptic insertion of AMPA receptors whereas late LTP additionally requires cAMP signaling and synthesis of new proteins (13). LTD at CA3-CA1 synapses can also be very long-lasting (14). LTD also depends on NMDA or metabotropic glutamate receptors and curiously, weak LTD can actually facilitate subsequent LTP (). The goal of this study was to overcome the time limitation of STDP experiments and investigate the late effects of STDP. To do this we used channelrhodopsins and light instead of electrodes to stimulate pre- and postsynaptic neurons and to readout the resulting changes in synaptic strength several days later.

Channelrhodopsins are ion channels that open in response to light, and since the discovery of channelrhodopsin-2 (15) have been widely used to stimulate neurons with light *in vitro* and *in vivo* (e.g. 16–18). In recent years, many channelrhodopsin variants have been discovered or engineered with varying kinetics and spectral sensitivity (e.g. 19, 20). We reasoned that using opsins sensitive to different wavelengths of light, we could circumvent the need for intracellular/patch-clamp recordings and optically induce 'no-patch' STDP. Here, we present a two-color method to stimulate precisely timed action potentials in defined subsets of CA3 and CA1 pyramidal neurons for optogenetic induction of STDP (oSTDP). Whereas oSTDP induced classical tLTP and tLTD in short-term patch-clamp experiments, the outcome after 3 days was strong tLTP regardless of the activation sequence. Our findings support the conclusion that the short and long-term consequences of STDP are different.

Results

Independently spiking neurons using ChrimsonR and CheRiff

To achieve our goal of independently spiking pre- and postsynaptic neurons, we used the red light sensitive ChrimsonR (19) and the blue/violet light-sensitive CheRiff (20). ChrimsonR-tdTomato was expressed in a small subset of CA3 pyramidal neurons by local virus injection and several CA1

neurons were electroporated with DNA encoding CheRiff-eGFP (Fig. 1A). In order to visualize CheRiff-expressing CA1 neurons (hereafter referred to as CheRiff-CA1 neurons) without activating them we also included DNA encoding mKate2 in the electroporation mix. We waited 7-10 days for expression of both channelrhodopsins before starting the experiments.

Given that the threshold for light-induced APs is not only opsin-dependent but also depends on expression levels and cell type, we performed a detailed analysis of the spectral sensitivity of ChrimsonR-CA3 and CheRiff-CA1 pyramidal neurons (*SI Appendix*, Fig. S1). According to this spectral analysis, we selected 405 nm (1.2 mW mm^{-2}) to activate CheRiff-CA1 neurons and 625 nm (8 mW mm^{-2}) to activate ChrimsonR-CA3 neurons. These intensities reliably and selectively evoked single action potentials/spikes in CA3 or CA1 pyramidal neurons using 1-2 ms flashes after 7-10 days expression (Fig. 1B). Although 405 nm light partially activates ChrimsonR, it did not spike ChrimsonR-CA3 neurons at 1 mW mm^{-2} (depolarization 0-3 mV, Fig. 1B). Importantly, red light (625 nm) caused no photocurrents in CheRiff-CA1 neurons at intensities up to 100 mW mm^{-2} nor did the yellow epifluorescence light used to visualize mKate2 (*SI Appendix,* Fig. S1). Thus, by using only yellow light (see Materials and Methods) we never inadvertently depolarized the postsynaptic CheRiff-CA1 neurons (i.e. only during pairing were cultures exposed to wavelengths less than 565 nm).

Optogenetic induction of spike-timing-dependent plasticity

We recorded excitatory postsynaptic currents (EPSCs) in CheRiff- or non-transfected CA1 neurons (hereafter referred to as NT-CA1 neurons) while optogenetically stimulating the approximately 30 ChrimsonR-CA3 neurons with single orange (594 nm, 2 ms) light flashes at 20 s intervals. As CA3 was outside the field of view of the objective when we patched the CA1 pyramidal neurons, we coupled the orange laser through the condenser (Fig. 1C and D). After five minutes baseline, we switched from voltage- to current-clamp mode. Single presynaptic ChrimsonR-CA3 spikes (300 flashes at 5 Hz, 2 ms duration, see methods) led or followed spike bursts by about 10 ms in the CheRiff-CA1 postsynaptic neurons (3 flashes at 50 Hz, 2 ms duration, *SI Appendix,* Fig. S2). Causal pairing (pre- before post-) induced tLTP (Fig, 1E, n = 12 experiments; p = 0.0002, Kolmogorov-Smirnov) whereas anti-causal pairing (post before pre) induced tLTD of ChrimsonR-CA3 to CheRiff-CA1 synapses (Fig. 1F, n = 11 experiments, p = 0.0009, Kolmogorov-Smirnov). There was a significant difference between causal and anti-causal groups (Fig 1G, p = 0.003, Kolmogorov-Smirnov). Importantly, the light stimulation used for causal pairing had no effect on synapses onto NT-CA1 neurons (median = 1.06, n = 6 experiments, p = 0.09, Kolmogorov-Smirnov, Fig 1G, *SI Appendix,* Fig. S2), indicating that oSTDP was specific to CheRiff-CA1 neurons and no plasticity was induced by the 5 Hz EPSPs alone. Evidently, using light to induce spikes in pre- and postsynaptic neurons produces oSTDP with similar timing rules as reported for this synapse when spikes were triggered by electrical stimulation (9, 10, 21–25).

Having established that oSTDP induces both tLTP and tLTD during patch-clamp experiments, we then developed a no-patch method to induce oSTDP and read-out synaptic input strength days later. Illumination towers, containing independently controlled, collimated, red (630 nm) and violet (405 nm) high-power LEDs were constructed to stimulate ChrimsonR-CA3 and CheRiff-CA1 neurons in the incubator (Fig. 2A). As we could not record EPSPs and spikes in the incubator we used the immediate early gene cFos that is upregulated in burst-spiking neurons (26) and in neurons that have undergone LTP (for review see 27) as a surrogate. We found no cFos-positive

ChrimsonR-CA3 neurons after causal pairing (9/9 slices) indicating that these neurons were not driven to burst by either the 630 nm light flashes (300 at 5 Hz, 8 mW mm^{-2}) or the 405 nm flashes (300 bursts of 3 at 50 Hz, 12 ms delay, 1 mW mm^{-2}). We validated this approach by observing that ChrimsonR-CA3 neurons expressed cFos when stimulated with bursts of three 630 nm flashes (300 bursts of 3 at 50 Hz, at 5 Hz, *SI Appendix,* Fig. S3) instead of single flashes. Thus, cFos is not expressed when pyramidal neurons fire 300 single spikes at 5 Hz but is expressed in neurons firing 300 bursts of 3 spikes, i.e. the ChrimsonR-CA3 neurons were not burst firing during no-patch oSTDP induction.

Likewise, 83% of CheRiff-CA1 neurons expressed cFos indicating they were directly driven to fire bursts of spikes during causal pairing as expected (7 slices: 30/36 neurons; Fig. 2E**,** *SI Appendix*, Fig. S4). Importantly, whether NT-CA1 neurons expressed cFos depended critically on the number of ChrimsonR-CA3 neurons in the slice. In 5 slices with 36-53 ChrimsonR-CA3 neurons, no NT-CA1 neurons expressed cFos (Fig. 2E**,** *SI Appendix*, Fig. S4). In 2 slices with 60-61 ChrimsonR-CA3 neurons, some NT-CA1 neurons showed cFos staining, and in 2 slices with 96 or more ChrimsonR-CA3 neurons, cFos staining was evident throughout the entire CA1 (*SI Appendix*, Fig. S4). Thus, we adjusted the amount of ChrimsonR virus injected to transduce ~30 CA3 neurons (e.g. Fig 1A).

The cFos expression pattern after in-incubator causal pairing, indicated the CheRiff and ChrimsonR neurons were being stimulated as expected, so we looked at the outcome of oSTDP 3 days later. Since baseline synaptic strength cannot be directly assessed, we compared the strength of ChrimsonR-CA3 to CheRiff-CA1 synapses with the strength of synapses onto neighboring NT-CA1 neurons. ChrimsonR-CA3 neurons were spiked with 594 nm laser flashes as described above and EPSCs were sequentially recorded from at least one CheRiff- and at least three NT-CA1 neurons per slice (Fig. 3A, B). The input strength calculated for each CheRiff-CA1 neuron, is the average EPSC slope of the CheRiff-CA1 neuron divided by the slope of the combined average EPSC recorded from the three or more NT-CA1 neurons in that slice (Fig. 3C). As expected, CheRiff-CA1 and neighboring NT-CA1 neurons received equivalent input from the ChrimsonR-CA3 neurons in control slices that were not previously stimulated with light, (Fig. 3D, no pairing; median = 0.91, mean = 1.04, CV = 0.53).

Input strength is potentiated three days after no-patch oSTDP

Three days after in-incubator causal pairing of EPSPs and spikes, the input strength from ChrimsonR-CA3 onto CheRiff-CA1 neurons was significantly stronger than in control 'no pairing' slices (Fig. 3D, +10 ms: median = 2.13, mean = 2.95, CV = 0.69; $P = 0.002$, Kolmogorov-Smirnov). Surprisingly, anti-causal pairing also resulted in stronger inputs three days later (Fig. 3D, -10 ms: median = 1.8, mean = 2.51, CV = 0.89; $P = 0.052$, Kolmogorov-Smirnov). The time interval between EPSPs and postsynaptic spikes was important, as input strength did not change significantly when Δt was 50 ms (Fig. 3D, +50 ms: median = 0.97, mean = 2.44, CV = 1.18; $P = 0.4$ Kolmogorov-Smirnov; -50 ms: median = 1.78, mean = 2.38, CV = 0.66; $P = 0.13$ Kolmogorov-Smirnov). Coincident activity of pre- and postsynaptic neurons was an absolute requirement for oSTDP as input strength was unchanged 3 days after burst firing the postsynaptic CheRiff-CA1 neurons alone (Fig. 3D, post only; $P = 0.6$ Kolmogorov-Smirnov). In previous studies, tLTP was associated with an immediate increase in postsynaptic excitability (28–30). Three days after oSTDP, we found no

differences in passive electrical parameters or excitability of CA1 neurons (*SI Appendix*, Fig. S5), indicating that the late effects of oSTDP were synaptic.

As for classical STDP (9, 10, 21, 22, 25), tLTP induced in the incubator was abolished when NMDA receptors were blocked during pairing (Fig. 3E, +CPP). Reducing the pairing frequency from 5 Hz to 0.1 Hz also prevented plasticity induction (Fig. 3E, 0.1 Hz), in line with previous studies (23).

It was unexpected and intriguing that anti-causal pairing of pre- and postsynaptic spikes did not decrease the input strength (Fig. 3D). As the stimulation was repeated every 200 ms, the tested timings covered all possible phase shifts between pre- and postsynaptic activity (Fig. 3G). The absence of tLTD was particularly surprising because during patch-clamp recordings, causal and anti-causal oSTDP clearly had opposite effects on EPSCs (Fig. 1E-G). As the distribution of input strengths following anti-causal pairing (-10 ms) appeared rather bimodal, we tested pairing protocols of different length in an attempt to uncover the expected depression (23). However, while 30 anti-causal pairings at 5 Hz did not induce any plasticity, all stronger protocols (100 to 500 repeats at 5 Hz) increased input strength (*SI Appendix*, Fig. S6).

We next investigated whether at a shorter time point after no-patch oSTDP, we would observe tLTD. As it takes time to settle the slices in the recording setup and sequentially patch the minimum of 4 neurons needed for one datapoint, the earliest time point after in-incubator oSTDP we could asses was 1-3 hours. Somewhat surprisingly, even at this earlier time, input strength was not significantly changed either by causal or anti-causal pairing, although a trend towards potentiation after causal pairing was apparent (*SI Appendix*, Fig. S7, -10 ms median = 1.04, P = 0.2 Kolmogorov-Smirnov; +10 ms median = 1.62, P = 0.56 Kolmogorov-Smirnov). Thus, tLTD was observed only during patch-clamp recordings and not later when the CA1 neurons were not patched during oSTDP induction.

We were intrigued that the strength of causally paired CA3-CA1 connections seemed to increase in the days following plasticity induction. We reasoned that after oSTDP, circuits containing potentiated synapses might develop higher levels of spontaneous spiking in the incubator, increasing re-activation of the synapses between the paired CA3 and CA1 neurons (30, 31). We either globally increased activity by completely changing the slice culture medium 3-4 hours after oSTDP or suppressed activity by including tetrodotoxin in the fresh medium. Both manipulations prevented potentiation (Fig. 4). These results suggest that the synaptic memory of a short episode of coincident activity was actively maintained and amplified in the cultures, pointing to a process that requires replay of activity patterns in the selected circuits.

Discussion

In previous studies, the usual requirement of impaling the postsynaptic neuron with a sharp electrode or using whole-cell or perforated patch recordings to induce STDP, has made it impossible to assess the late (i.e. days later) effects of STDP. In the present study, we demonstrated that (1) the opsins CheRiff and ChrimsonR can be used to independently spike CA3 and CA1 neurons, (2) during patch-clamp recordings optogenetic causal pairing of pre- and postsynaptic spiking induces tLTP whereas anti-causal pairing induces tLTD, and (3) the long-term consequence of pairing closely apposed pre- and postsynaptic spikes is potentiation regardless of the timing sequence.

As during short-term patch-clamp recordings oSTDP follows the same timing rules as demonstrated in many studies of electrically-induced STDP (9–11, 32, 33), we surmise that optically- and electrically-induced spiking are not fundamentally different. Late oSTDP differs from the short-term effects observed during patch-clamp recordings as tLTD is no longer observed. Late oSTDP is however, similar to short-term electrical STDP in several important respects. Late oSTDP remains sensitive to spike timing, as no potentiation occurs when postsynaptic neurons spike 50 ms after the EPSP (Fig 3G). At this time, GABA-A currents from feed-forward inhibition are strongly activated in CA1 neurons (34) and may reduce the synaptic calcium influx necessary for potentiation as has been demonstrated for back-propagating action potentials (35). Late tLTP also depends on NMDA receptors as is well established for electrode-induced STDP (21), strongly suggesting that elevated intracellular [Ca^{2+}] in the postsynaptic neuron is essential. A further similarity of late oSTDP to electrode-induced STDP is the strong frequency-dependence of oSTDP (23): At a pairing repetition rate of 5 Hz, tLTP was observed, but not when the pairing rate was reduced to 0.1 Hz.

To us, the most surprising result is the apparent lack of tLTD three days after oSTDP induction. Neither increasing nor decreasing the number of anti-causal pairing repetitions unmasked a late tLTD. Nor was tLTD apparent at the earliest time window (1-3 hours) feasible after no-patch oSTDP. The fact that we did not detect statistically significant differences in input strength at this early time point is consistent with a slow, activity-dependent enhancement of tLTP. We hypothesize that slight differences in synaptic strength or excitability, induced by the only structured activity that was ever provided in these slice cultures, were enhanced over time by an active process. That the 'memory' of causal pairing is erased when spontaneous activity is disrupted supports this hypothesis, but obtaining direct evidence will require the continuous monitoring of the circuit activity over several days. Interestingly, maintenance and consolidation of memories also require ongoing activity and NMDA receptors (36–38).

In addition to time of readout, there are several caveats to comparing the early and late outcome of the oSTDP experiments. The temperature of the slices during the induction were different, 33 °C vs 37 °C. At 35 °C we had only two stable recordings of six so resorted to the lower temperature. We used slice culture medium to perform the early oSTDP patch-clamp experiments but had to omit the horse serum, which was present in the incubator-stimulated slices. Another, possibly the most important difference is that in early oSTDP experiments, the postsynaptic neurons had whole-cell patch-clamp electrodes attached. Might it be that tLTD occurs only in neurons 'damaged' and with contents dialyzed with recording electrodes? We induced oSTDP 5-10 minutes after obtaining whole-cell access, as it is well known that washout of important cellular components prevents plasticity induction (39). Additional evidence against the hypothesis that early tLTD is purely due to washout are STDP studies using sharp electrodes or perforated patch recordings, that have reported both tLTD and tLTP (32, 33). Still, it is possible that the act of patching the postsynaptic neuron compromises tLTP, and biases synapses towards depression (40).

Another caveat is that we could not verify that every CA1 neuron received synaptic input or that every CheRiff-CA1 neuron spiked as expected while being stimulated in the incubator. What if the opsin expressing neurons either failed to fire action potentials during no-patch oSTDP induction or fired multiple action potentials? Extensive experience has taught us that very short (1-2 ms) light flashes with an intensity range from threshold until about 5x spike threshold will reliably evoke single spikes in neurons expressing relatively fast channelrhodopsins. We therefore used very short

flashes of calibrated intensity set to ~2x average spike threshold (determined for CheRiff-CA1 and ChrimsonR-CA3 neurons at 7 days after transfection) for the induction of oSTDP. Additionally, we verified during oSTDP readout that every CheRiff-CA1 neuron analyzed indeed spiked at this intensity (see methods). Fewer than 5% of all CheRiff-CA1 neurons failed to spike at this intensity and were discarded. Of the remaining CheRiff-CA1 neurons, only 6% fired two spikes to the single light flash. On the presynaptic side, we selected the lowest laser intensity tested that evoked at least -20 pA EPSCs in the non-transfected neurons, to bias the synapses being assayed toward those made by ChrimsonR-CA3 neurons with low spike thresholds i.e. those synapses most likely being activated in the incubator. The cFos staining results suggest that CA3 stimulation was not driving bursting throughout CA1 at least in the samples slices. That the early effects of oSTDP replicated the classical asymmetric STDP window, strongly argues against optogenetic artifacts being solely responsible for the difference in early and late effects. As channelrhodopsins are distributed in the plasma membrane, it could even be argued that optical generation of spikes is more physiological than somatic current injection; spiking normally arises from distributed synaptically-induced depolarization of dendrites and spines. Indeed, experiments pairing mossy fiber with CA3 synaptic inputs induces tLTP or tLTD of the CA3-CA3 synapses without spiking of the postsynaptic CA3 neuron (41). Likewise, at CA3-CA1 Schaffer collateral synapses tLTP can occur without postsynaptic spikes (42). Thus, if CheRiff-CA1 cells occasionally missed spiking and only depolarized in response to the violet light flashes, tLTD and tLTP would still be the expected outcome.

While the majority of STDP studies report both potentiation and depression, ‘LTP-only’ STDP windows have been observed at human hippocampal, human and rat neocortical synapses (43, 44) and in mouse hippocampus (23), most commonly in the presence of increased dopamine (33, 43). If presynaptic activity is paired with prolonged postsynaptic bursts (plateau potentials), the timing window for Schaffer collateral potentiation can be extended to several seconds in the causal and anti-causal direction (45). Explanations for these discrepant outcomes of early oSTDP abound, but we speculate that if synaptic strength was assessed after several days, the outcome of repeated coincident activity may always be potentiation regardless of the exact temporal sequence. Conservation of total synaptic weight may be provided by heterosynaptic LTD or via generalized downscaling processes (46).

Materials and Methods

Rat organotypic hippocampal slice cultures

Wistar rats were housed and bred at the University Medical Center Hamburg-Eppendorf (UKE) animal facility and sacrificed according to German Law (Tierschutzgesetz der Bundesrepublik Deutschland, TierSchG) with approval from the Behörde für Gesundheit und Verbraucherschutz Hamburg and the animal care committee of the UKE. The procedure for organotypic cultures was modified from Stoppini et al. (47), using media without antibiotics. Detailed protocol was previously published in (48). After opsins were expressing, great care was taken to protect the cultures from wavelengths of light below 560 nm to prevent unintentional co-activation of ChrimsonR and CheRiff-expressing neurons. Handling and normal medium changes (2/3, twice per week) were under dim yellow light, which may directly depolarize ChrimsonR but not CheRiff expressing neurons (Osram LUMILUX CHIP control T8).

Viral vector-based transduction

The plasmid pAAV-syn-ChrimsonR-TdTomato, a kind gift from Edward Boyden (Addgene # 59171), was packaged into AAV viral particles with serotype Rh10 (7.22*1013 vg ml^{-1}) at the Vector Core facility of the University Medical Center Hamburg-Eppendorf. One µl was loaded into a micropipette with the tip broken to ~10 µm diameter. Slice cultures (12-14 DIV) were transferred into sterile pre-warmed (37 °C) HEPES-buffered solution containing: NaCl (145 mM, Sigma; S5886-500G), HEPES (10 mM, Sigma; H4034-100G), D-glucose (25 mM, Sigma; G7528-250G), KCl (2.5 mM, Fluka; 60121-1L), $MgCl_2$ (1 mM, Fluka; 63020-1L), $CaCl_2$ (2 mM, Honeywell; 21114-1L), pH 7.4, 318 mOsm kg^{-1}. The virus-containing pipette was inserted into CA3 and a small bolus was pressure-ejected using 3-5 pressure pulses (Picospritzer: 2 bar, 80-100 ms). Our aim was to transduce approximately 30 CA3 neurons in CA3 with ChrimsonR. A detailed description of the viral transduction has been published (49).

Single-cell electroporation

Plasmids used for electroporation were: 1) pAAV-hsyn-CheRiff-eGFP (Addgene #51697), 0.5 ng ml^{-1}, kindly provided by Adam Cohen; 2) pCI-syn-mKate2, 10 ng ml^{-1} was created by replacing GCaMP3 in pCI-syn-GCaMP3 using hindIII and NotI with mKate2-N from pmKate2-N (Evrogen cat. # FP182). Plasmids were diluted in intracellular solution containing: K-gluconate (135 mM, Sigma; G4500-100G), EGTA (0.2 mM, Sigma-Aldrich; E0396-10G), HEPES (10 mM, Sigma; H4034-100G), $MgCl_2$ (4 mM, Fluka; 63020-1L), Na_2-ATP (4 mM, Aldrich; A26209-1G), Na-GTP (0.4 mM, Sigma; G8877-100MG), Na_2-phosphocreatine (10 mM, Sigma; P7936-1G), ascorbate (3 mM, Sigma; A5960-100G), pH 7.2, 295 mOsm kg^{-1}. Slice cultures were transferred to a sterile microscope chamber filled with sterile 37°C HEPES-buffered solution (see viral vector-based transduction) either right after AAV injection or 1 day later. Pipettes (10-15 MΩ, World Precision Instruments; TW150F-3) were filled with the plasmid mixture and several pyramidal neurons in CA1 were touched and electroporated using an Axoporator (25 pulses, -12 V, 500 µs, 50 Hz). A detailed description of the electroporation procedure has been published (50).

CheRiff and ChrimsonR characterization

For characterizing responses to multiple wavelengths, we used a pE-4000 CoolLED (CoolLED Ltd., s/n CP0180) with an additional filter for 550 nm (555±20 nm) coupled through the dual camera port of the electrophysiology setup described below. Light intensities in the specimen plane were measured using a 918D-ST-UV sensor and 1936R power meter (Newport). Light flashes (1 ms, low to high intensity) were delivered every 20 s with one minute between wavelength sequences. Whole cell currents were recorded (see electrophysiology below) with synaptic transmission and action potentials blocked by CPPene (10 µM, Tocris bioscience; 1265), NBQX (10 µM, Tocris bioscience; 1044), picrotoxin (100 µM, Sigma; P1675-1G) and tetrodotoxin (1 µM, HelloBio; HB1035). Seven CA1 (CheRiff) and eleven CA3 (ChrimsonR) neurons were recorded from to obtain n = 4 responses at each wavelength/intensity combination. Average peak light-evoked currents were determined and plotted (*SI Appendix*, Fig. S1) using a self-written MATLAB code.

Electrophysiology and optogenetic stimulation

The setup is based on an Olympus BX61WI microscope fitted with Dodt contrast, epifluorescence and CCD-camera (DMK23U274, The Imaging Source) on a dual camera port (see Fig. 1C). For light stimulation through the objective an LED combiner (Mightex Systems, wavelengths 625, 530, 470, 405 nm) was coupled via 1 mm multimode fiber and collimator (Thorlabs) mounted on one of

the camera ports. A 40x water immersion objective (Plan-Apochromat 1.0 NA DIC VIS-IR, Zeiss, illuminated field ø 557 µm) or a 10x water immersion objective (UMPlanFL 0.30 NA W, Olympus, illuminated field ø 2.65 mm) were used. Light intensities through the objectives were measured in the specimen plane using a calibrated power meter (LaserCheck, Coherent or 918D-ST-UV sensor / 1936R power meter, Newport). To locally activate CA3 neurons, the orange (594) laser beam of an Omicron Light Hub was coupled to an optical fiber fitted with a collimator (Thorlabs) mounted on a lockable swing arm. This construction allowed us to point the laser beam at different angles through the center of the back aperture of the oil immersion condenser (NA 1.4, Olympus) to locally illuminate neurons in CA3 away (~1.5 mm) from the optical axis, with high intensity and little light scattering (Fig 1C). After final laser positioning, the stage was not moved and CA1 neurons within the single field of view were recorded from.

Whole-cell patch-clamp recordings were performed using an Axopatch 200B (Axon Instruments, Inc.) amplifier, National Instruments A/D boards and Ephus software (51). All recordings, except the experiments in Fig. 1E-G and 2B-D (see next section), were performed blind to slice treatment at 30°C (in-line heater, Warner Instruments) in artificial cerebral spinal fluid containing: NaCl (119 mM, Sigma; S5886-500G), $NaHCO_3$ (26.2 mM, Sigma; S5761-500G), D-glucose (11 mM, Sigma; G7528-250G), KCl (2.5 mM, Fluka; 60121-1L), NaH_2PO_4 (1 mM, Sigma; S5011-100G), $MgCl_2$ (4 mM, Fluka; 63020-1L), $CaCl_2$ (4 mM, Honeywell; 21114-1L), pH 7.4, ~310 mOsm kg^{-1}, saturated with humidified 95% O_2 / 5% CO_2. Patch electrodes (3-4 MΩ, World Precision Instruments; 1B150F-3) were filled with the same intracellular solution used for electroporation (above). Liquid junction potential was measured (-14.1 to -14.4 mV) and corrected. CA1 pyramidal neurons were patched under the 40x water immersion objective and voltage-clamped at -70 mV (LJP corrected). A test pulse (-5 mV, 200 ms) was applied at the start of every sweep. Series resistance (Rs) was less than 20 MΩ, did not change more than 30% and was not compensated in voltage clamp. In current clamp we used the bridge balance compensation.

Optogenetic induction of spike-timing dependent plasticity during whole-cell recordings

Eight to eleven days after virus injection and electroporation of ChrimsonR and CheRiff, slices were transferred to the electrophysiology setup and perfused with slice culture medium (described above) without horse serum (replaced with MEM), supplemented with D-serine (30 µM, Tocris Bioscience; 0226) and diluted slightly to give ~308 mOsm kg^{-1} (33 °C, saturated with humidified 95% O_2 / 5% CO_2). The LJP was measured and corrected (-15.3 mV). The medium (50 ml) was recycled during the experiment and changed every 4 hours or every 4 slices, whichever came first. With the 594 nm laser positioned to stimulate ChrimsonR-CA3 neurons, a CA1 neuron was patched and EPSCs were recorded (every 20s) at -65.3 mV (LJP corrected) where inhibitory currents were clearly outward. Laser intensity was set to evoke EPSCs of approximately -100 pA (range -50 pA to -200 pA). Baseline EPSCs were recorded for up to 5 minutes after break-in. The 10x objective was carefully moved into position to maximize the area of the slice illuminated and the amplifier was switched to current clamp to allow spiking of the CA1 neuron during paired optogenetic stimulation. To induce plasticity, stimulation of ChrimsonR-CA3 neurons 300 x 2 ms pulses at 5 Hz (594 nm laser at baseline intensity plus simultaneous red LED stimulation in the CA1 (625 nm, 2 mW mm^{-2})) was combined with bursts of 3 violet LED stimuli in CA1 (405 nm, 2 ms, 50 Hz, 1 mW mm^{-2}) to activate CheRiff-CA1 neurons. We set the delay between orange/red and the last or first of the violet light flashes of -10 ms or +10 ms for anti-causal and causal pairing, respectively but after 9 experiments observed the actual median delay from the last action potential (AP) to EPSP onset was -14.2 ms during anti-causal pairing and from EPSP onset to the first AP was 6.8 ms during causal pairing. We therefore advanced the red/orange flash by 2 ms relative to the violet

flash during the remaining experiments obtaining a more symmetrical median timing of -12.4 ms during anti-causal and 8.8 ms during causal pairing. After pairing CA3 and CA1 stimulation, EPSCs (0.05 Hz orange laser flashes) were recorded for an additional 25 minutes. The EPSC slope was measured using a self-written script in MATLAB. To determine whether tLTP or tLTD occurred in an individual experiment the baseline slopes (black points in Fig. 1E) and the slopes measured in the last 5 minutes (magenta points in Fig. 1E) were compared with Kolmogorov-Smirnov tests (significance $p < 0.05$). A Kolmogorov-Smirnov test was used to test whether the normalized EPSC slopes were different between the anti-causal and causally paired groups. Plots and statistical analyses were performed using Matlab and GraphPad Prism.

In-incubator oSTDP, read-out and analysis

For all 'no patch' oSTDP experiments, read-out and analysis were performed by an investigator blinded to the induction protocol. Unblinding occurred after the target n for a particular group was reached (~ 7 CheRiff neurons from 4 slices). Experimental groups were inter-mixed to ensure blinding and to mitigate the possibility of unexpected batch or time-dependent factors influencing the outcome resulting in uneven n's between treatment groups.

We waited 7-10 days to allow stable expression of ChrimsonR and CheRiff. One to three days before in-incubator light stimulation, the slice cultures (placed singly on the inserts) were transferred to and centered in a 35 mm culture dish. Where indicated CPPene (1 µM, Fig. 3E) was added to the slice culture medium the day before. The closed petri dish containing the centered slice culture was placed in an LED illumination tower constructed from 30 mm optical bench parts (Thorlabs) that was inside a dedicated incubator (Fig. 2A). The tower contained an injection-molded reflector (Roithner LaserTechnik, 10034) to collimate the 630 nm LED (Cree XP-E red) and an aspheric condenser lens (Thorlabs ACL2520U-A) to collimate the 405 nm LED (Roschwege Star-UV405-03-00-00). The LEDs were powered and controlled from outside the incubator by a two-channel Grass S8800 stimulator, two constant-current drivers (RECOM RCD-24-1.20) and a timer. LED power was adjusted to give 1.2 mW mm^{-2} for 405 nm and 8 mW mm^{-2} for 630 nm inside the petri dish in the specimen plane. Considering the spread in actual spike-burst delay (Fig. 1G), Δt was set to +52, +12, -8, or -48 ms to produce EPSP-spike delays of ~+50 ms, +10 ms, -10 ms and -50 ms, respectively (light pulse duration 2 ms). Pairing frequency was 5 Hz or 0.1 Hz. Paired activation was repeated 300 times unless otherwise indicated. 'Non-paired' cultures were handled identically but no light stimulation was given. After pairing, each petri dish was marked with only a letter code and date/time of pairing. Where indicated (Fig. 4), 3-4 hours after pairing fresh pre-warmed medium with 1 µM tetrodotoxin (TTX) was pipetted on top of the membrane to immediately silence neurons in the slice. The medium under the slice was then aspirated, replaced with the TTX containing medium and the medium on top of the slice was removed before returning the slice to the incubator, so that the slice was again exposed to the humidified incubator atmosphere. Two days later the TTX was washed 3 times with fresh medium and the slices returned to the incubator until the following day when they were recorded from. For the medium change condition, cultures were handled identically except the medium never contained TTX.

One hour or 3 days after in-incubator stimulation, slices were transferred by the blinded investigator to the electrophysiology setup with on/off axis stimulation and perfused with ACSF at 30 °C as described above. The slice was positioned so that CheRiff-CA1 neurons as well as at least 5 non-transfected CA1 pyramidal neurons were in the field of view of the 40x objective and camera (Fig. 3A). The 594 nm laser was positioned to activate the ChrimsonR-CA3 neurons (see above). Whole-cell patch-clamp recordings were sequentially made from 3 to 4 NT-CA1 pyramidal neurons and 1 to 5 CheRiff-CA1 pyramidal neurons in a pseudo-random sequence without moving the stage to ensure constant CA3 stimulation (holding potential -70 mV to ensure separation between EPSCs

and IPSCs). While still in cell-attached mode, CA1 neurons were illuminated with a single 405 nm light flash (1 ms, 1.2 mW mm^{-2}). None of the 250 NT-CA1 neurons spiked. Of 212 fluorescent CheRiff-CA1 neurons, 96% spiked in response to the violet flash, 190 fired a single spike (89.6%) and 13 fired 2-3 spikes (6.1%). The recordings were immediately discontinued from the remaining 9 neurons that did not spike (4.25%).

After break-in, orange laser flashes (594 nm, 20 s interval) stimulated ChrimsonR-CA3 neurons to evoke EPSCs in the CA1 neurons. EPSC onset was typically 6 to 8 ms after the stimulation. If the delay to EPSC onset was 13 ms or longer they were assumed polysynaptic and not analyzed. Ten EPSCs were recorded at each of 3 laser intensities from each CA1 neuron (when spontaneous events obscured the EPSCs a few more sweeps were collected). The middle intensity was set to evoke an EPSC of about -100 to -300 pA in the first recording from a given slice. The same 3 intensities were used for all neurons in a given slice. Importantly, we found no correlation between laser intensity and the amount of LTP induced. At the end of each recording, we injected a series of current steps to assess cellular excitability. Cells without pyramidal-like firing patterns (i.e. high AP frequency, large amplitude after-hyperpolarization) were eliminated from the analysis.

For analysis, we selected the EPSCs from one laser intensity per slice. The selected intensity evoked the most similar EPSC slopes that were at least 20 pA in three non-transfected cells (usually the lowest laser intensity). Individual sweeps with spontaneous EPSCs/IPSCs within 10 ms of the stimulation were suppressed. If fewer than 4 sweeps remained at the selected laser intensity, the recording was discarded. A custom Matlab routine averaged the EPSCs, detected the (first) peak and the 20-60% slope (Fig. 3C). If the time of the peak varied by more than 5 ms between neurons, we suspected a mixture of mono and polysynaptic responses and the slice was excluded. Input strength was defined as the slope from each CheRiff-CA1 neuron divided by the slope of the average EPSC from all NT-CA1 neurons in the given slice. GraphPad Prism 8 was used for statistics and to create plots.

Immunohistochemistry

Ninety minutes after stimulation, slices were fixed (30 minutes, ice-cold 4% paraformaldehyde in PBS). Slices were washed in PBS (3 x 10 min) and blocked (2 hours 5% donor horse serum, 0.3 % TritonTM X-100 in PBS at RT) and then incubated overnight with the primary antibody (4° C, rabbit anti-cFos, Santa Cruz Biotechnology, Inc., sc-52, 1:500) in carrier solution (1 % Bovine serum albumin, 0.3 % TritonTM X-100 in PBS). Next day slices were washed 3 times in PBS and incubated at RT for 2 hours with a secondary antibody (Alexa Fluor 488 goat anti-rabbit, Life Technologies, A11008; or Alexa Fluor 568 goat anti-rabbit, Life Technologies, A11011) at 1:1000 in carrier solution (same as above) and afterwards washed again (3 x 10 min) in PBS and mounted with Shandon Immu-Mount (Thermo Scientific; 9990402).

Confocal microscopy

An Olympus F1000 confocal microscope and 20x objective (UPLSAPO 0.85 NA, Olympus) were used with the laser/filter sets designed for Alexa 488, Alexa 546 and Alexa 568 as appropriate. Z-series images were obtained using a 3 µm z-step at a 1024x1024-pixel resolution scanning at 12.5 µs per pixel. Image parameters were adjusted for the red and green channels and were kept constant throughout. Fiji/ImageJ (52) was used to project the z-series and overlay channels.

Acknowledgments

We would like to thank Mark van Rossum for critical comments on the manuscript. Iris Ohmert, Sabine Graf, Torsten Renz, Dirk Lubrich, Lennart Sobirey, Paul Lamothe and Ingke Braren (UKE Vector facility) provided important technical support. CheRiff was a gift from Adam Cohen, ChrimsonR was a gift from Edward Boyden. The first spectral characterization of ChrimsonR-expressing neurons in slice cultures was performed by Katie Ferguson and Longzhi Tan during the 2014 Neurobiology Course at MBL in Woods Hole. Funding was received from: the Landesforschungsförderung Hamburg; the Deutsche Forschungsgemeinschaft (DFG) grants SPP 1665 220176618, SPP1926 315380903, SFB 936 178316478, SFB 1328 335447717, FOR 2419 278170285, Emmy Noether 259979908 and the European Research Council (ERC-StG 714762).

References

1. S. Song, K. D. Miller, L. F. Abbott, Competitive Hebbian learning through spike-timing-dependent synaptic plasticity. *Nat. Neurosci.* **3**, 919–926 (2000).

2. W. Gerstner, R. Kempter, J. L. van Hemmen, H. Wagner, A neuronal learning rule for sub-millisecond temporal coding. *Nature* **383**, 76–81 (1996).

3. M. C. van Rossum, G. Q. Bi, G. G. Turrigiano, Stable Hebbian learning from spike timing-dependent plasticity. *J. Neurosci.* **20**, 8812–8821 (2000).

4. R. P. Costa, R. C. Froemke, P. J. Sjöström, M. C. W. van Rossum, Unified pre- and postsynaptic long-term plasticity enables reliable and flexible learning. *Elife* (2015) https:/doi.org/10.7554/eLife.09457.

5. T. Masquelier, R. Guyonneau, S. J. Thorpe, Competitive STDP-Based Spike Pattern Learning. *Neural Comput.* **21**, 1259–1276 (2009).

6. T. Serrano-Gotarredona, T. Masquelier, T. Prodromakis, G. Indiveri, B. Linares-Barranco, STDP and STDP variations with memristors for spiking neuromorphic learning systems. *Front. Neurosci.* **7** (2013).

7. M. Mozafari, M. Ganjtabesh, A. Nowzari-Dalini, T. Masquelier, SpykeTorch: Efficient Simulation of Convolutional Spiking Neural Networks With at Most One Spike per Neuron. *Front. Neurosci.* **13**, 625 (2019).

8. A. Diamond, M. Schmuker, T. Nowotny, An unsupervised neuromorphic clustering algorithm. *Biol. Cybern.* **113**, 423–437 (2019).

9. D. Debanne, B. H. Gähwiler, S. M. Thompson, Long-term synaptic plasticity between pairs of individual CA3 pyramidal cells in rat hippocampal slice cultures. *J. Physiol.* **507**, 237–247 (1998).

10. G. Q. Bi, M. M. Poo, Synaptic modifications in cultured hippocampal neurons: dependence on spike timing, synaptic strength, and postsynaptic cell type. *J. Neurosci.* **18**, 10464–10472 (1998).

11. H. Markram, J. Lübke, M. Frotscher, B. Sakmann, Regulation of synaptic efficacy by coincidence of postsynaptic APs and EPSPs. *Science (80-.).* **275**, 213–215 (1997).

12. T. V Bliss, T. Lomo, Long-lasting potentiation of synaptic transmission in the dentate area of the anaesthetized rabbit following stimulation of the perforant path. *J. Physiol.* **232**, 331–56 (1973).

13. U. Frey, Y. Huang, E. Kandel, Effects of cAMP simulate a late stage of LTP in

hippocampal CA1 neurons. *Science (80-.).* **260**, 1661–1664 (1993).

14. V. Doyère, M. L. Errington, S. Laroche, T. V. P. Bliss, Low-frequency trains of paired stimuli induce long-term depression in area CA1 but not in dentate gyrus of the intact rat. *Hippocampus* **6**, 52–57 (1996).

15. G. Nagel, *et al.*, Channelrhodopsin-2, a directly light-gated cation-selective membrane channel. *Proc. Natl. Acad. Sci.* **100**, 13940–13945 (2003).

16. E. S. Boyden, F. Zhang, E. Bamberg, G. Nagel, K. Deisseroth, Millisecond-timescale, genetically targeted optical control of neural activity. *Nat. Neurosci.* **8**, 1263–1268 (2005).

17. D. Huber, *et al.*, Sparse optical microstimulation in barrel cortex drives learned behaviour in freely moving mice. *Nature* **451**, 61–4 (2008).

18. A. R. Adamantidis, F. Zhang, A. M. Aravanis, K. Deisseroth, L. de Lecea, Neural substrates of awakening probed with optogenetic control of hypocretin neurons. *Nature* **450**, 420–424 (2007).

19. N. C. Klapoetke, *et al.*, Independent optical excitation of distinct neural populations. *Nat. Methods* **11**, 338–46 (2014).

20. D. R. Hochbaum, *et al.*, All-optical electrophysiology in mammalian neurons using engineered microbial rhodopsins. *Nat. Methods* **11**, 825–833 (2014).

21. T. Nevian, B. Sakmann, Spine Ca2+ Signaling in Spike-Timing-Dependent Plasticity. *J. Neurosci.* **26**, 11001–11013 (2006).

22. C. M. Tigaret, V. Olivo, J. H. L. P. Sadowski, M. C. Ashby, J. R. Mellor, Coordinated activation of distinct Ca2+ sources and metabotropic glutamate receptors encodes Hebbian synaptic plasticity. *Nat. Commun.* **7**, 10289 (2016).

23. G. M. Wittenberg, S. S. Wang, Malleability of spike-timing-dependent plasticity at the CA3-CA1 synapse. *J. Neurosci.* **26**, 6610–6617 (2006).

24. N. Holbro, A. Grunditz, J. S. Wiegert, T. G. Oertner, AMPA receptors gate spine Ca(2+) transients and spike-timing-dependent potentiation. *Proc Natl Acad Sci U S A* **107**, 15975–15980 (2010).

25. E. Edelmann, *et al.*, Theta Burst Firing Recruits BDNF Release and Signaling in Postsynaptic CA1 Neurons in Spike-Timing-Dependent LTP. *Neuron* **86**, 1041–1054 (2015).

26. P. Schoenenberger, D. Gerosa, T. G. Oertner, Temporal control of immediate early gene induction by light. *PLoS One* **4**, e8185 (2009).

27. J. Jaworski, K. Kalita, E. Knapska, c-Fos and neuronal plasticity: the aftermath of Kaczmarek's theory. *Acta Neurobiol. Exp. (Wars).* **78**, 287–296 (2018).

28. A. Frick, J. Magee, D. Johnston, LTP is accompanied by an enhanced local excitability of pyramidal neuron dendrites. *Nat. Neurosci.* **7**, 126–135 (2004).

29. D. Debanne, M.-M. Poo, Spike-timing dependent plasticity beyond synapse - pre- and post-synaptic plasticity of intrinsic neuronal excitability. *Front. Synaptic Neurosci.* **2**, 21 (2010).

30. D. Debanne, Y. Inglebert, M. Russier, Plasticity of intrinsic neuronal excitability. *Curr. Opin. Neurobiol.* **54**, 73–82 (2019).

31. J. H. L. P. Sadowski, M. W. Jones, J. R. Mellor, Sharp-Wave Ripples Orchestrate the Induction of Synaptic Plasticity during Reactivation of Place Cell Firing Patterns in the Hippocampus. *Cell Rep.* **14**, 1916–1929 (2016).

32. R. M. Meredith, A. M. Floyer-Lea, O. Paulsen, Maturation of long-term potentiation induction rules in rodent hippocampus: role of GABAergic inhibition. *J. Neurosci.* **23**, 11142–11146 (2003).

33. J.-C. Zhang, P.-M. Lau, G.-Q. Bi, Gain in sensitivity and loss in temporal contrast of STDP by dopaminergic modulation at hippocampal synapses. *Proc. Natl. Acad. Sci. U. S. A.* **106**, 13028–13033 (2009).

34. D. D. Samulack, J.-C. Lacaille, Hyperpolarizing synaptic potentials evoked in CA1 pyramidal cells by glutamate stimulation of interneurons from the oriens/alveus border of rat hippocampal slices. II. sensitivity to GABA antagonists. *Hippocampus* **3**, 345–358 (1993).

35. J. J. Marlin, A. G. Carter, GABA-A receptor inhibition of local calcium signaling in spines and dendrites. *J. Neurosci.* **34**, 15898–911 (2014).

36. Z. Cui, *et al.*, Inducible and Reversible NR1 Knockout Reveals Crucial Role of the NMDA Receptor in Preserving Remote Memories in the Brain. *Neuron* **41**, 781–793 (2004).

37. E. Shimizu, Y. P. Tang, C. Rampon, J. Z. Tsien, NMDA receptor-dependent synaptic reinforcement as a crucial process for memory consolidation. *Science* **290**, 1170–4 (2000).

38. P. Smolen, D. A. Baxter, J. H. Byrne, How can memories last for days, years, or a lifetime? Proposed mechanisms for maintaining synaptic potentiation and memory. *Learn. Mem.* **26**, 133–150 (2019).

39. R. Malinow, R. W. Tsien, Presynaptic enhancement shown by whole-cell recordings of long-term potentiation in hippocampal slices. *Nature* **346**, 177–180 (1990).

40. P. J. Sjöström, G. G. Turrigiano, S. B. Nelson, Rate, timing, and cooperativity jointly determine cortical synaptic plasticity. *Neuron* **32**, 1149–1164 (2001).

41. F. Brandalise, U. Gerber, Mossy fiber-evoked subthreshold responses induce timing-dependent plasticity at hippocampal CA3 recurrent synapses. *Proc. Natl. Acad. Sci.* **111**, 4303–4308 (2014).

42. J. Hardie, N. Spruston, Synaptic Depolarization Is More Effective Than Back-Propagating Action Potentials During Induction of Associative Long-Term Potentiation in Hippocampal Pyramidal Neurons. *J. Neurosci.* **29**, 3233–3241 (2009).

43. Z. Brzosko, W. Schultz, O. Paulsen, Retroactive modulation of spike timing-dependent plasticity by dopamine. *Elife* **4**, e09685 (2015).

44. G. Testa-Silva, Human synapses show a wide temporal window for spike-timing-dependent plasticity. *Front. Synaptic Neurosci.* (2010) https:/doi.org/10.3389/fnsyn.2010.00012 (September 14, 2019).

45. K. C. Bittner, A. D. Milstein, C. Grienberger, S. Romani, J. C. Magee, Behavioral time

scale synaptic plasticity underlies CA1 place fields. *Science* **357**, 1033–1036 (2017).

46. G. G. Turrigiano, The dialectic of Hebb and homeostasis. *Philos. Trans. R. Soc. B Biol. Sci.* **372**, 20160258 (2017).

47. L. Stoppini, P. A. Buchs, D. Muller, A simple method for organotypic cultures of nervous tissue. *J. Neurosci. Methods* **37**, 173–82 (1991).

48. C. E. Gee, I. Ohmert, J. S. Wiegert, T. G. Oertner, Preparation of Slice Cultures from Rodent Hippocampus. *Cold Spring Harb. Protoc.* **2017**, 126–130 (2017).

49. J. S. Wiegert, C. E. Gee, T. G. Oertner, Viral Vector-Based Transduction of Slice Cultures. *Cold Spring Harb. Protoc.* **2017**, 131–134 (2017).

50. J. S. Wiegert, C. E. Gee, T. G. Oertner, Single-Cell Electroporation of Neurons. *Cold Spring Harb. Protoc.* **2017**, 135–138 (2017).

51. B. A. Suter, *et al.*, Ephus: multipurpose data acquisition software for neuroscience experiments. *Front. Neural Circuits* **4**, 100 (2010).

52. J. Schindelin, *et al.*, Fiji: an open-source platform for biological-image analysis. *Nat. Methods* **9**, 676–682 (2012).

Figures and Tables

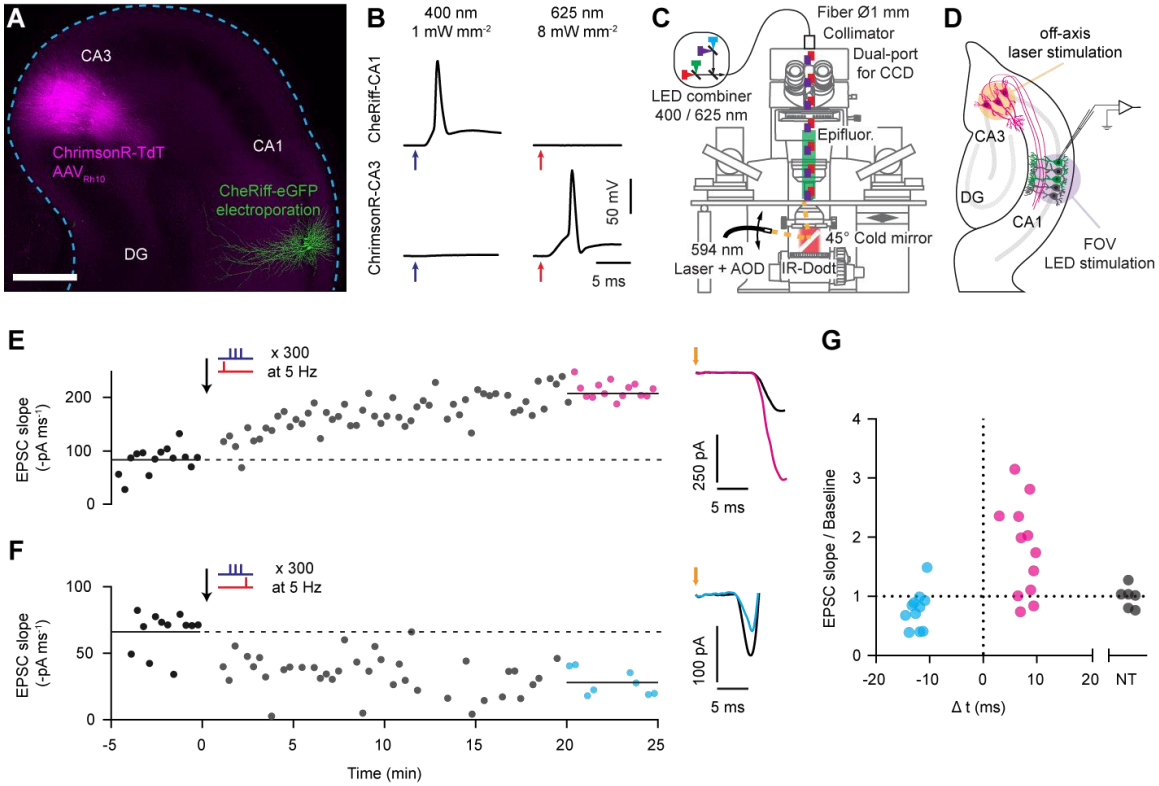

Figure 1. Optogenetic induction of spike-timing-dependent plasticity (oSTDP). A, Organotypic hippocampal slice culture, with ~30 CA3 neurons expressing ChrimsonR (magenta) and 3 CA1 neurons expressing CheRiff (green). Scale bar 500 µm. **B,** Example membrane responses of CheRiff-CA1 (upper traces) and ChrimsonR-CA3 (lower traces) neurons to 405 nm (violet arrows) and 625 nm (red arrows) light flashes (2 ms). Note that the CheRiff-CA1 neuron spikes and the ChrimsonR-CA3 neuron only slightly depolarizes in response to 405 nm light whereas in response to 625 nm light the ChrimsonR-CA3 neuron spikes and there is no response in the CheRiff-CA1 neuron. **C,** Diagram of the electrophysiological recording setup with on-axis LED and off-axis laser stimulation. **D,** Diagram of an organotypic hippocampal slice in the recording chamber. **E,** The slope of excitatory postsynaptic currents (EPSCs) recorded from one CheRiff-CA1 neuron in response to laser stimulation of ChrimsonR-CA3 neurons at baseline (black points) and after (grey and magenta points) causal pairing (t = 0, black arrow, one red (625 nm) and 12 ms later three violet (400 nm, 50 Hz) light flashes repeated 300 times at 5 Hz). At right are the averaged EPSCs from the black and magenta points, orange arrow shows time of laser flash to stimulate ChrimsonR-CA3 neurons. The magenta points were significantly potentiated relative to the baseline (black points), $p < 0.0001$, Kolmogorov-Smirnov. **F,** As in **E** but after anti-casual stimulation (three 400 nm light flashes preceded the 625 nm light flash by 8 ms). The cyan points were significantly depressed relative to baseline (black points), $p = 0.003$, Kolmogorov-Smirnov **G,** Average EPSC slope 20-25 minutes after oSTDP induction normalized to baseline from experiments as in **E** (magenta, n = 12) and **F** (cyan, n = 11), Δt is the actual EPSP-spike timing interval observed during the pairing (c.f. *SI Appendix Fig. S2*). NT, non-transfected neurons from slices subjected to causal pairing stimulation (n = 6). Magenta vs cyan points $p = 0.003$, Kolmogorov-Smirnov.

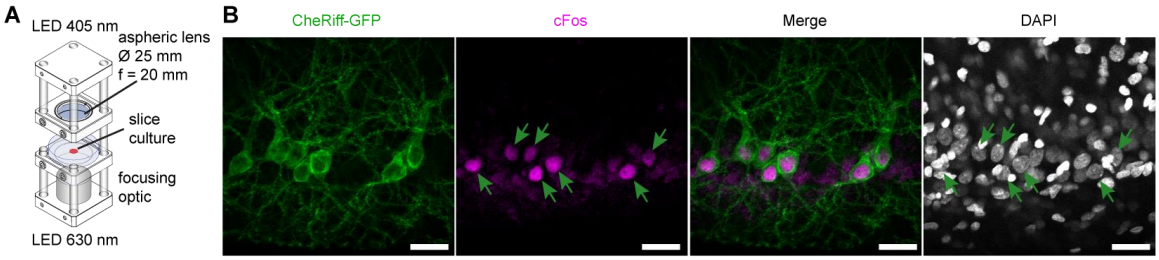

Figure 2. Activity-dependent cFos expression in CheRiff-CA1 neurons following in-incubator no-patch oSTDP. A, Diagram of the device used for in-incubator optogenetic stimulation of ChrimsonR-CA3 and CheRiff-CA1 neurons in hippocampal slice cultures. **B,** Expression of cFos in the CA1 region of a slice culture fixed 1.5 hours after causal in-incubator oSTDP stimulation. Confocal image stacks of CheRiff-CA1 neurons (green), anti-cFos (magenta) and overlay. At right are the DAPI stained nuclei. Green arrows point to nuclei of the CheRiff-CA1 neurons. Scale bars 50 µm.

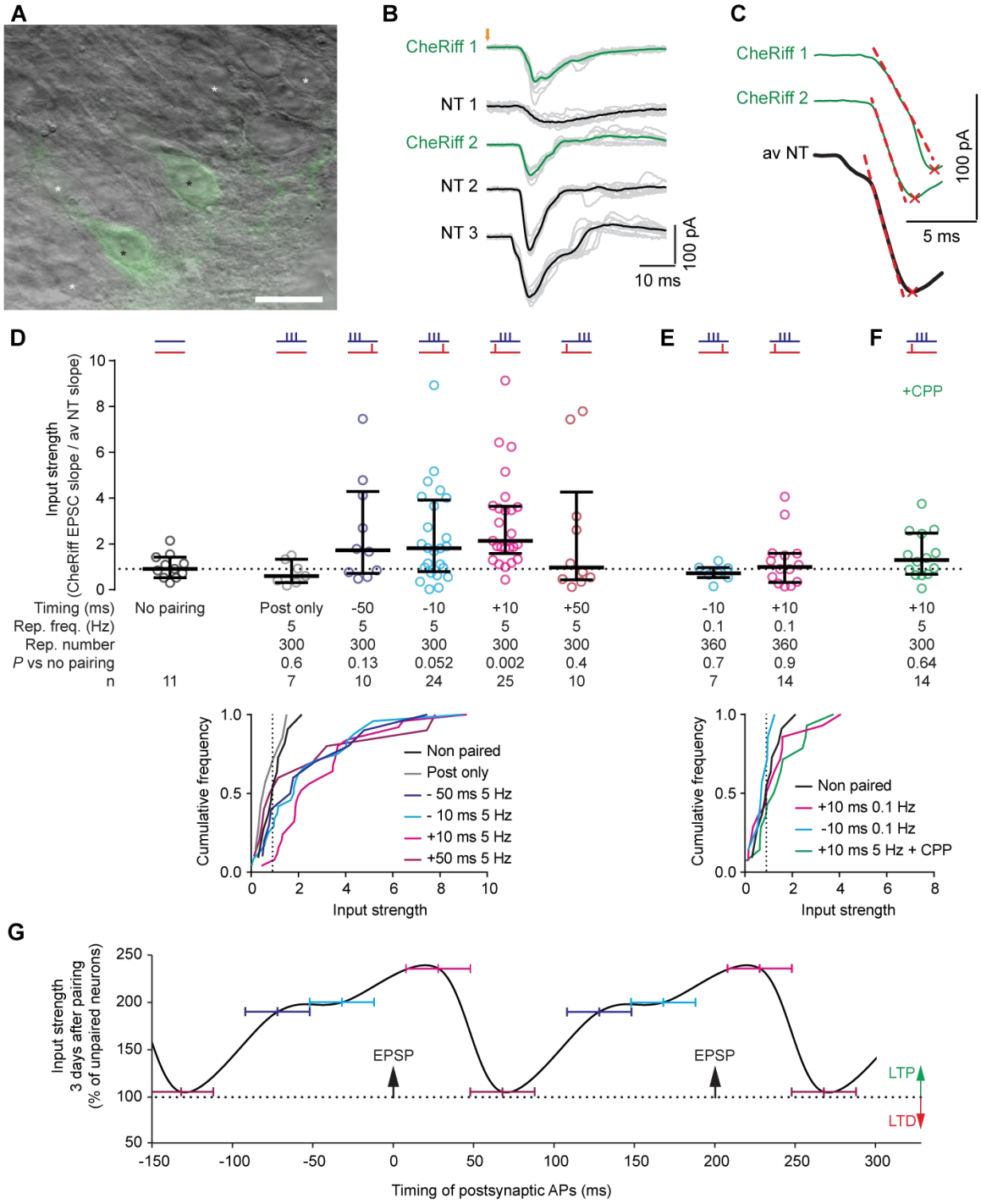

Figure 3 Three days after oSTDP only potentiation is evident. A, Dodt-contrast image (40x objective) of CA1 region with overlaid epifluorescence image. Black asterisks: CheRiff expressing CA1 pyramidal neurons; white asterisks: non-transfected CA1 pyramidal neurons suitable for recording. Note that the actual field of view is about 30% larger. Scale bar 25 µm. **B,** Laser stimulation (orange arrow, 1 ms, 594 nm) of ChrimsonR-CA3 neurons evoked excitatory postsynaptic currents (EPSCs) in CA1 neurons of a control (no oSTDP pairing) slice. EPSCs recorded sequentially from CheRiff-CA1 pyramidal neurons (green, average of 10 grey individual

EPSCs) and at least three non-transfected (NT) CA1 neurons (black average of 10 grey individual EPSCs). **C,** Automatically-detected EPSC peak (red x) and slope (dashed red line, 20-60% peak). EPSCs from NT neurons were averaged before determining the NT slope. **D,** Normalized input strength of CheRiff-CA1 neurons recorded from control (no pairing) slices and slices 3 days after pairing. At top red and violet ticks indicate order of pre- and postsynaptic stimulation, respectively. Plotted are individual data points, median and 25-75% interquartile range and cumulative frequency distributions (below). The dotted line is the median input strength onto CheRiff-CA1 neurons of the non-paired slices (median = 0.91). 'Timing' is the target interval between start of the EPSC and the first or last postsynaptic spike. 'Rep. freq.' is the pairing repetition frequency. 'Rep. num.' is the number of pairings. *P* values (Kolmogorov-Smirnov) are vs no pairing, n number of CheRiff-CA1 neurons in each experiment. **E,** As in **D** except the repetition frequency was reduced to 0.1 Hz for one hour. In all cumulative frequency plots the non-paired group was added as reference. **F,** As in **D** but the NMDA antagonist CPPene was in the culture medium during pairing (+CPP, 1 µM). **G,** Median input strength (% no pairing median) plotted relative to the light-induced EPSPs (arrows) and action potential timings (vertical ticks on colored bars) during oSTDP pairing (data from **E,** brown +50 ms, violet -50 ms, cyan -10 ms, magenta +10 ms). Two cycles (of 300) at 5 Hz are illustrated.

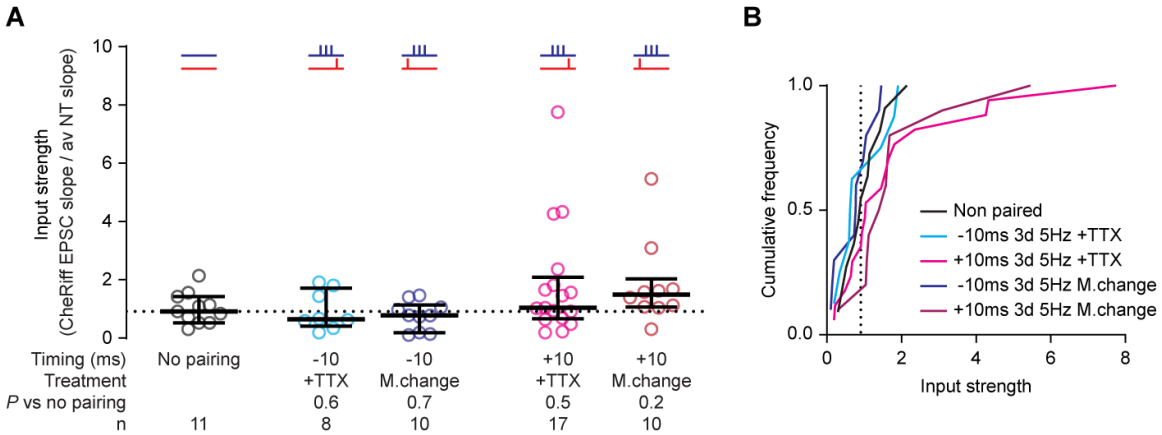

Figure 4. Activity in the paired pathway is essential for long term potentiation. A, Normalized input strength of CheRiff-CA1 neurons recorded from causally or anti-causally (300 rep at 5 Hz) paired slices 3 days later. The no pairing group is reproduced from Fig 3D. Three to four hours after oSTDP medium was changed (M. change) to increase global activity or activity was blocked with tetrodotoxin (+TTX, 1 µM). Two days later medium was changed again and TTX washed off. Plotted are individual data points, median and 25-75% interquartile range. P values (Kolmogorov-Smirnov) are vs no pairing group. **B,** Cumulative frequency distributions of **A**.

SI Appendix

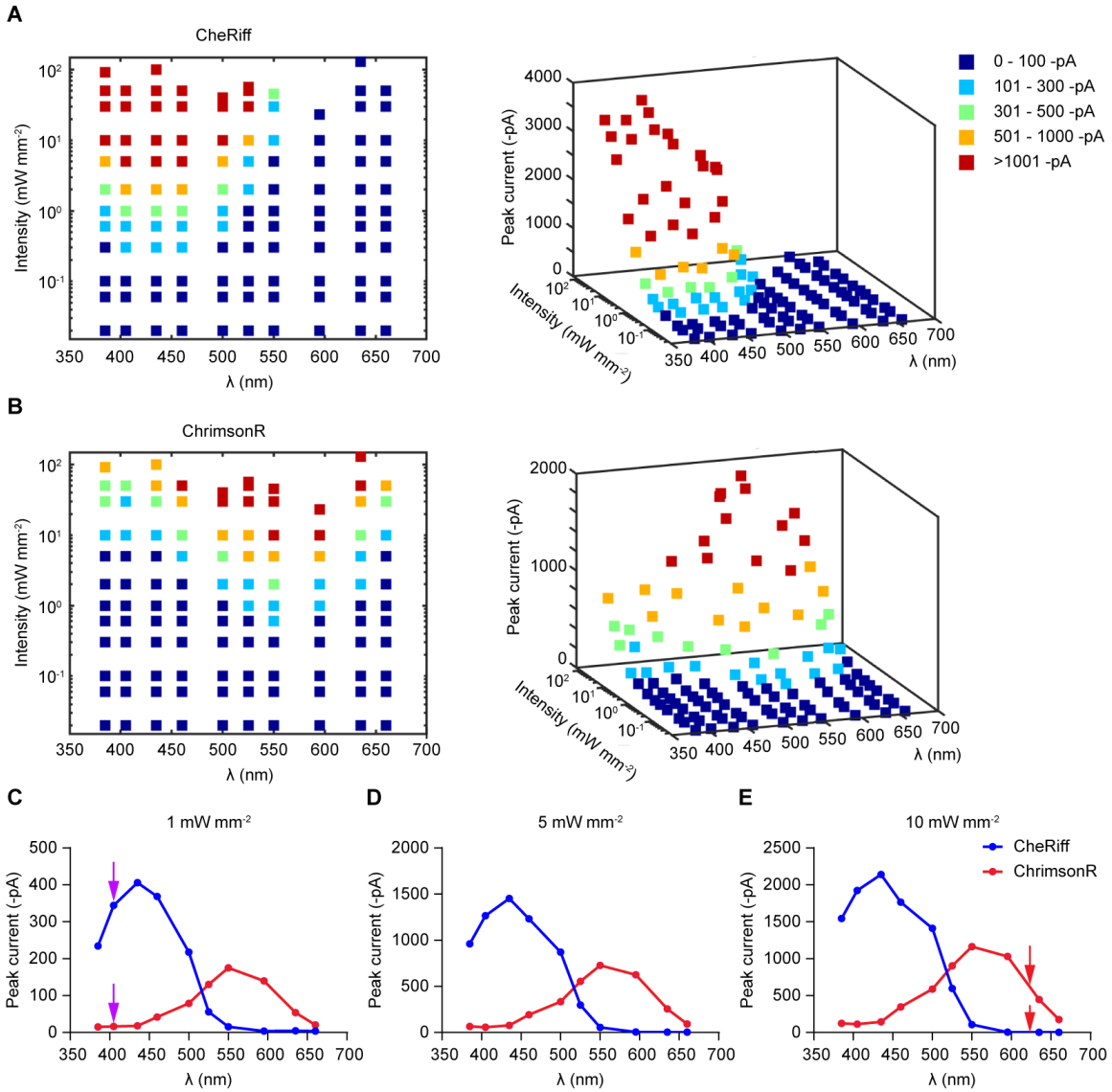

Supplementary Figure S1. CheRiff and ChrimsonR functional characterization. A, B, Average (n = 4 cells per point) light evoked EPSC peaks from CheRiff-CA1 neurons (electroporated) and ChrimsonR-CA3 neurons (AAV transduced) in response to stimulation with different wavelengths at different intensities. Color code indicates average peak current amplitude. Note that CheRiff-CA1 neurons were completely non-responsive to light with wavelengths longer than 550 nm and ChrimsonR-CA3 neurons were only modestly responsive to 405 nm light. Peak current vs wavelength at: **C,** 1 mW mm^{-2}, **D,** 5 mW mm^{-2} and **E,** 10 mW mm^{-2} for CheRiff-CA1 and ChrimsonR-CA3 neurons. Note different y-axis scales. Arrows indicate wavelengths/intensities used for oSTDP induction.

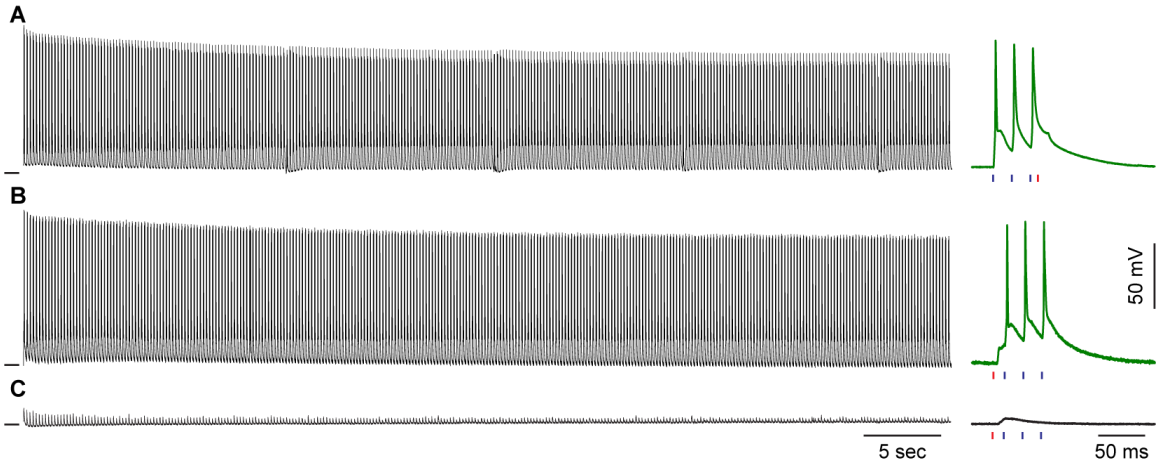

Supplementary Figure S2. Sample membrane responses of CA1 neurons during causal and anti-causal optical spike-timing-dependent plasticity pairing. A, Full recording (left) and time-expanded response (right) of a CheRiff-CA1 neuron during anti-causal pairing (-10 ms: 3 violet flashes at 50 Hz and 1 red flash 8 ms after, repeated 300x at 5 Hz). Note the EPSP following three spikes (right). Black ticks at far left indicate -70 mV. **B,** as in **A**, CheRiff-CA1 neuron during causal pairing (+10 ms: 1 red flash and 3 violet flashes at 50 Hz 12 ms after). Note the EPSP precedes the three spikes (right). **C,** Membrane voltage response of a non-transfected CA1 neuron during causal pairing. Note the EPSPs and absence of spikes.

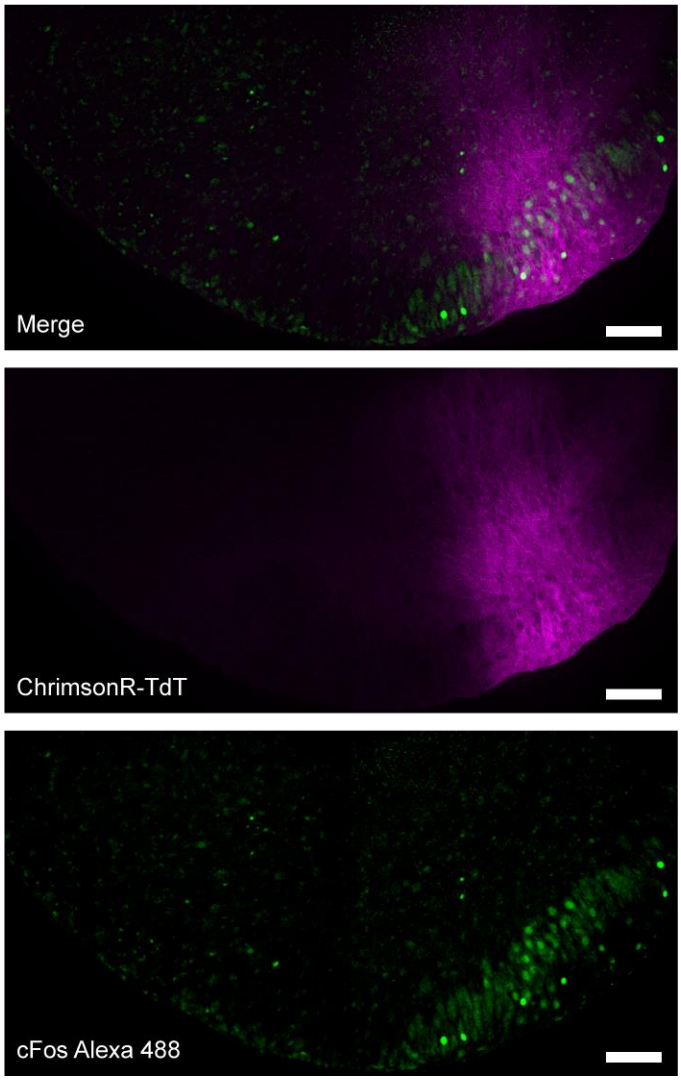

Supplementary Figure S3. CA3 neurons express cFos after burst firing. Confocal images of CA3 area of a hippocampal slice culture fixed 1.5 hours after burst stimulation (Blocked synaptic transmission: 1 µM CPPene, 100 µM Picrotoxin, 10 µM NBQX; red light: 3 flashes at 50 Hz repeated 300x at 5 Hz, 630 nm, 8 mW mm^{-2}). The ChrimsonR-tdTomato channel (magenta) is a minimum-intensity projection to visualize transfected neurons and a median-intensity projection was used for anti-cFos immunostaining (green). Approximately half of the burst-stimulated ChrimsonR-CA3 neurons were cFos-positive as were several non-transduced spontaneously active CA3 neurons. Scale bars 100 µm.

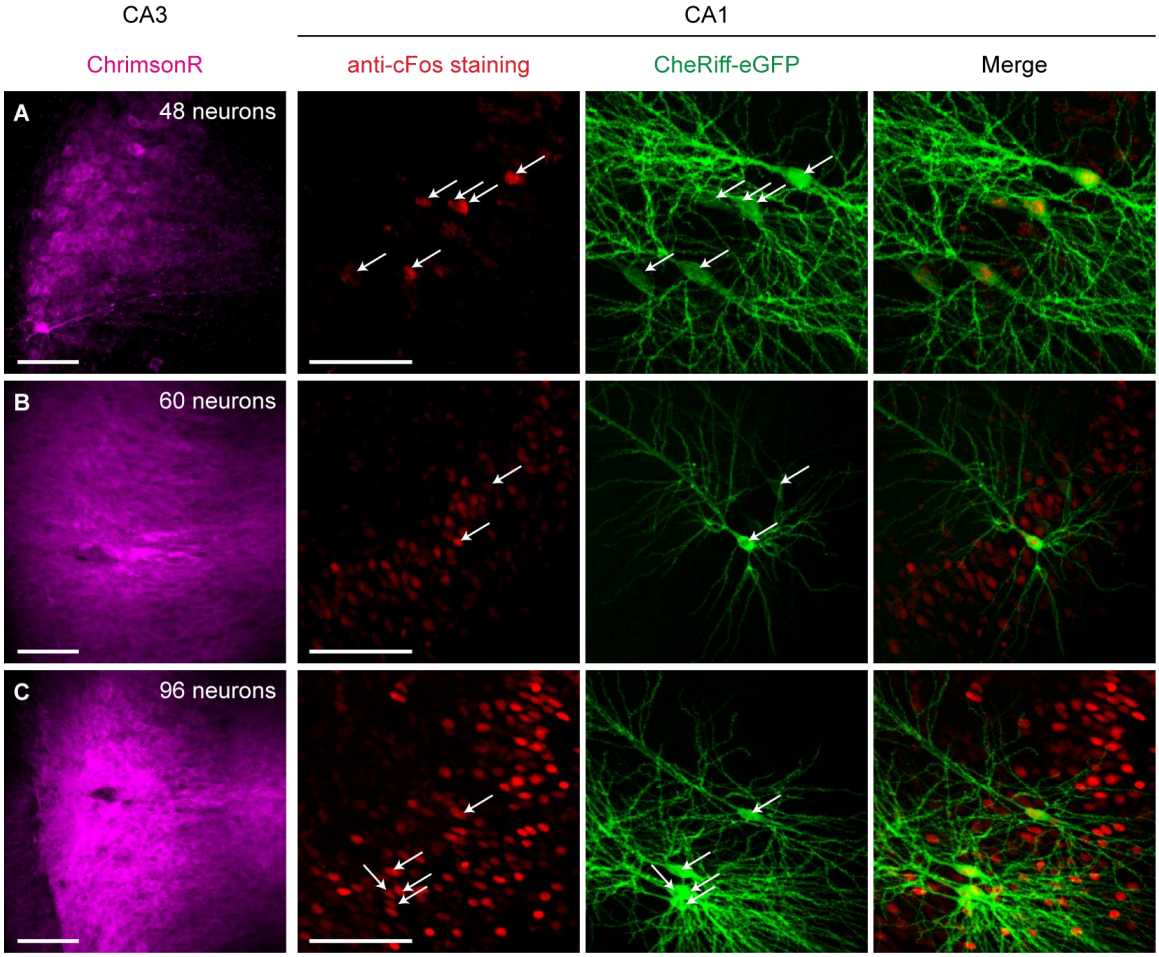

Supplementary Figure S4. cFos expression pattern after causal pairing vs number of ChrimsonR-CA3 neurons. Confocal images (average intensity projection) of CA3 and CA1 areas in a given slice culture. White arrows are showing the soma of CheRiff-CA1 neurons. Scale bars 100 µm. **A,** Expected cFos expression pattern in CA1 after causal pairing: Only directly light stimulated CheRiff-CA1 express cFos (5 out of 6). **B and C,** Number of ChrimsonR-CA3 neurons enough to induce complex spiking in CA1, which lead to cFos expression in NT-CA1 neurons.

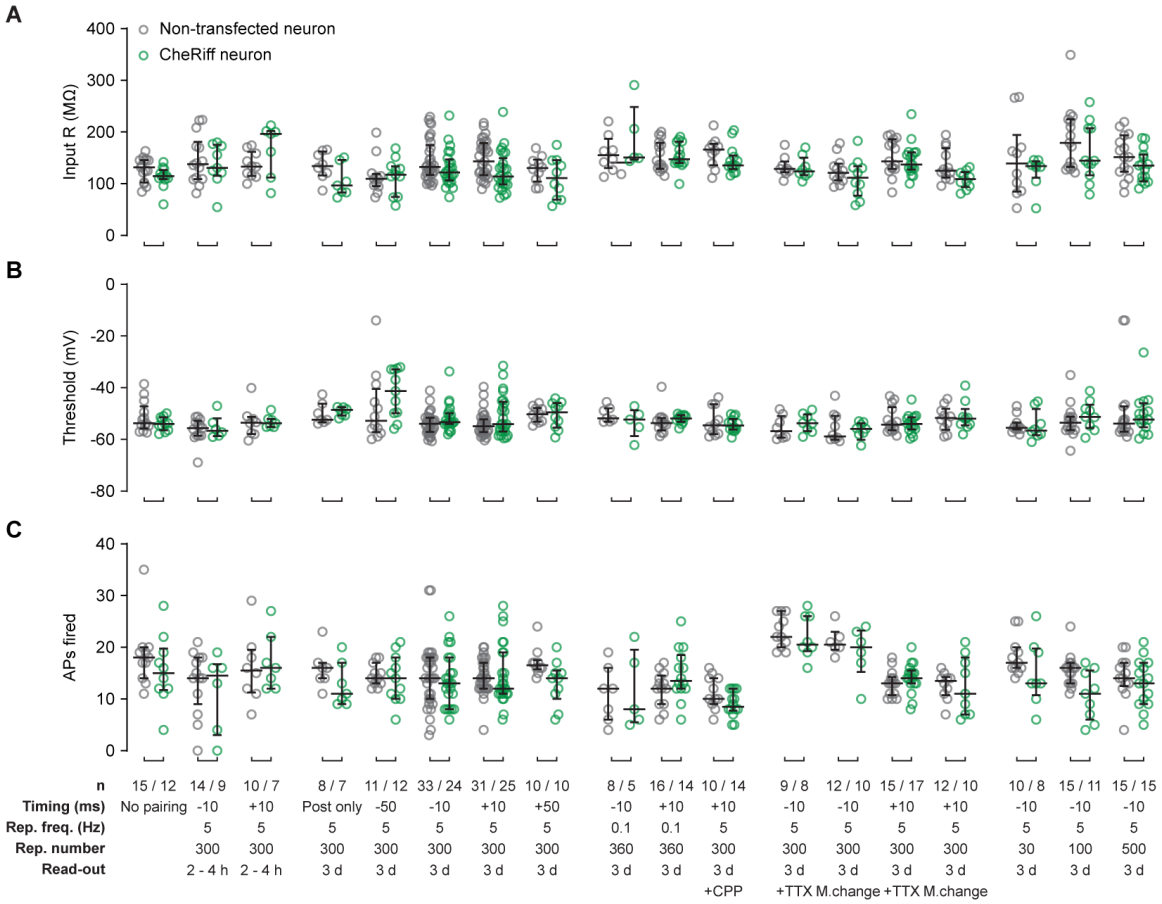

Supplementary Figure S5. Comparison of passive and active cell parameters of CheRiff-CA1 and neighboring NT-CA1 neurons from experiments in Fig. 3 and Fig. 4. A, Input resistance of all CheRiff-CA1 and NT neurons. **B,** Action potential threshold. **C,** Numbers of action potentials fired in response to a 400 pA current step. There were no significant differences between NT and CheRiff-CA1 neurons in any of the treatment groups (Kolmogorov-Smirnov). +CPP, 1 µM CPPene during oSTDP; +TTX, 1 µM tetrodotoxin 4-48 h after oSTDP; M. change, medium changed 4 and 48 h after oSTDP. *n* given as number of NT-CA1 / CheRiff-CA1 neurons.

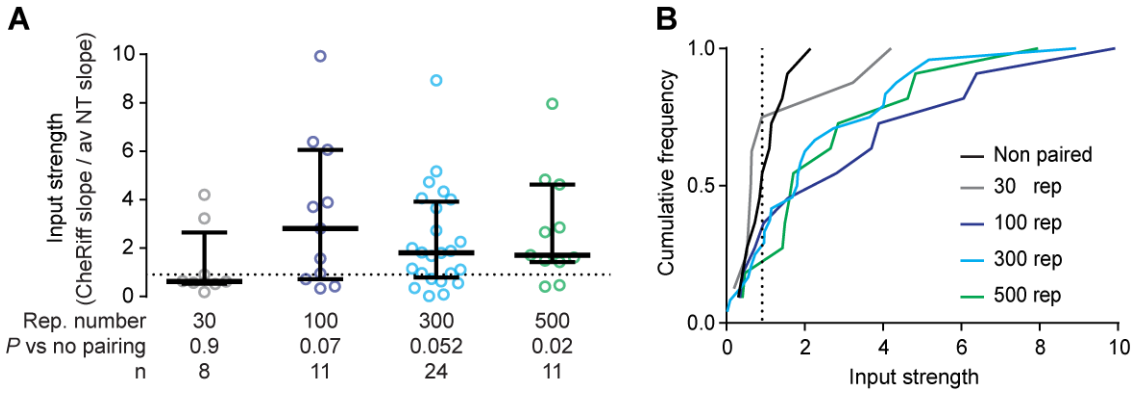

Supplementary Figure S6. Anti-causal pairing with different number of repeats still results in potentiation. A, Anti-causal pairing was applied as in Fig. 3 but the number of pairings at 5 Hz was varied as indicated (Rep. number). **B,** Cumulative frequency distributions. The non-paired and 300 repetition groups are duplicated from Fig. 3 for comparison. *P* values (Kolmogorov-Smirnov) are vs non-paired group from Fig.3.

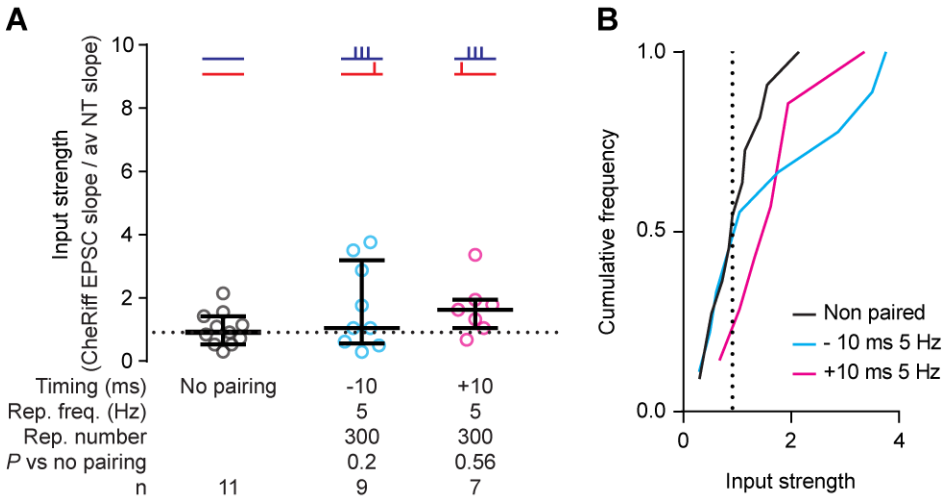

Supplementary Figure S7. Input strength is not changed 3 hours after oSTDP induction. A, Normalized input strength of CheRiff-CA1 neurons recorded from causally or anti-causally (300 rep at 5 Hz) paired slices approximately 3 hours later. The no pairing group is reproduced from Fig 3D. **B,** Cumulative frequency distributions. *P* values (Kolmogorov-Smirnov) are vs non-paired group.